Geophysical Research Letters

RESEARCH LETTER
10.1029/2018GL080350

Reassessing the Role of the Indo-Pacific in the Ocean's Global Overturning Circulation

Emily R. Newsom[1] **and Andrew F. Thompson**[1]

[1]Environmental Science and Engineering, California Institute of Technology, Pasadena, CA, USA

Key Points:
- Constraints on overturning pathways, based on global surface buoyancy forcing, are tested in comprehensive climate model
- Indo-Pacific air-sea fluxes require zonal asymmetries in the global overturning circulation
- Active low-latitude, Indo-Pacific surface controls on global overturning dynamics are proposed

Supporting Information:
- Supporting Information S1

Correspondence to:
E. R. Newsom,
enewsom@caltech.edu

Citation:
Newsom, E. R., & Thompson, A. F. (2018). Reassessing the role of the Indo-Pacific in the ocean's global overturning circulation. *Geophysical Research Letters*, *45*, 12,422–12,431. https://doi.org/10.1029/2018GL080350

Received 5 SEP 2018
Accepted 29 OCT 2018
Accepted article online 1 NOV 2018
Published online 28 NOV 2018

Abstract Surface buoyancy fluxes in the Southern and North Atlantic Oceans are presumed to disproportionately influence the ocean's residual global overturning circulation (GOC) with respect to those in the Indo-Pacific. Here, this assumption is challenged through an assessment of global buoyancy transport in the Community Earth System Model 1.0, which reveals that the steady state GOC is equally constrained by surface buoyancy flux everywhere. Further, an unacknowledged aspect of the GOC is demonstrated: it transports buoyancy from where it is gained at the surface, predominately in the Indo-Pacific, to where it is lost, predominately in the Atlantic and Southern Oceans. This global buoyancy transport requires zonal structure in the GOC, linking the Atlantic and Indo-Pacific within the Southern Ocean, asymmetry and interbasin coupling absent from many conceptual descriptions of overturning dynamics. These results compel a more nuanced appreciation for an Indo-Pacific influence in GOC evolution.

Plain Language Summary The great *conveyor belt* of global currents that transit the global ocean—the global overturning circulation—carry with them heat, freshwater, and dissolved gases that are essential to Earth's climate. Changes in heating and cooling of the ocean surface, or changes to patterns of precipitation, are known to influence this global-scale circulation, but a full understanding of the response remains incomplete. In this study, we develop a new technique to study the global overturning circulation. Our methods use the spatial patterns of ocean surface processes, for example, heating and cooling, precipitation and evaporation, to infer circulation behaviors deep in the ocean's interior. Historically, deep ocean behaviors were thought to be influenced by surface processes occurring at the high latitudes. Here, using this new technique, we find that surface processes at the low latitudes of the Indo-Pacific Oceans are equally essential in determining the strength and structure of the global overturning circulation. As a consequence, the climate that we experience at Earth's surface may depend far more heavily on the processes occurring at the equatorial Indo-Pacific Ocean surface than often assumed.

1. Introduction

The global overturning circulation (GOC) is a complex global circuit that connects all the major basins of the ocean (Broecker, 1991; Gordon, 1986; Lumpkin & Speer, 2007; Schmitz, 1996; Talley, 2013). Its state—the spatial pattern, sense, and strength with which waters circulate the interior—regulates the exchange of heat, carbon, and other essential chemicals between the ocean and atmosphere. As such, a robust theory for global climate evolution relies upon a robust understanding of what controls the GOC.

The three-dimensional complexity of the GOC has been appreciated for decades; however, its governing dynamics have largely been explored in simplified ocean models (e.g., Gnanadesikan, 1999; Munk, 1966; Stommel, 1961, and many others). In general, such frameworks strive to remain simple enough that the response to a perturbation can be mechanistically understood while still including all fundamental ocean processes. This idealized approach has afforded an increasingly nuanced assessment of the controls on the global ocean state, yet in doing so, has relied on several key assumptions. Recurrent since Munk (1966) is the notion that the GOC is highly sensitive to surface buoyancy fluxes at high latitudes, particularly the North Atlantic and the Southern Oceans (Bell, 2015; Gnanadesikan, 1999; Jansen & Nadeau, 2016; Klinger & Marotzke, 1999; Marotzke & Klinger, 2000; Nikurashin & Vallis, 2011, 2012; Radko & Kamenkovich, 2011; Samelson, 2009; Wolfe & Cessi, 2011). In other words, these unique regions exert a strong control on ocean overturning from *above*. In contrast, the Indian and Pacific Oceans are expected to influence global overturning through interior mixing processes; these basins are assumed to control the GOC from *below* (e.g., Ferrari et al., 2014; Nikurashin &

Vallis, 2011; Thompson et al., 2016). The assumed roles of each region in the global system are either implicit in one-dimensional (Munk, 1966) or zonally averaged frameworks (e.g., Gnanadesikan, 1999; Nikurashin & Vallis, 2011, 2012; Wolfe & Cessi, 2011), or explicit in those that include two northern basins (e.g., Ferrari et al., 2017; Thompson et al., 2016). Critically, these expectations beget a third implicit assumption: the GOC is neither controlled nor constrained by low-latitude surface buoyancy fluxes and upper ocean dynamics in the Indo-Pacific. In practice, the models discussed to treat the low-latitude surface as an infinite reservoir of heat and fresh water through relaxation to prescribed boundary conditions; the majority omit any representation of the subtropical gyres dynamics, which physically separate the low-latitude surface ocean from the deep global overturning below. Despite a marked evolution in conceptual descriptions of the GOC, from a *conveyor belt* paced by North Atlantic Deep Water (NADW) formation rates (Broecker, 1987, 1991), to a more complex global loop (e.g., Lumpkin & Speer, 2007; Talley, 2013), dependent on both NADW formation rates and Southern Ocean buoyancy fluxes (e.g., Ferrari et al., 2014; Thompson et al., 2016), an assumption persists that low-latitude surface fluxes will passively and indefinitely adjust to equilibrate high-latitude forcing and interior dynamics.

In this study, we explore the possibility that the low-latitude Indo-Pacific may also influence the GOC from above. Our motivation comes from the global surface buoyancy flux distribution itself, which combines the effect of surface heat and freshwater fluxes on seawater density. For example, Figure 1 illustrates the surface flux distribution from an unforced simulation in Community Earth System Model (CESM 1.0), described further in section 2. This model simulates buoyancy loss from the high-latitude Atlantic and Southern Oceans, where NADW and Antarctic bottom waters are formed and buoyancy gain in the Southern Ocean, where deep waters upwell and are modified by the atmosphere. This pattern complies to expectations: these respective processes are unique to each region due to numerous aspects of planetary and continental geometry or topography, which constrain ocean-atmosphere coupling (as argued by, e.g., Czaja, 2009; De Boer et al., 2008; Ferreira et al., 2010, 2017; Jones et al., 2017; Marshall & Radko, 2003; Nilsson et al., 2013; Toggweiler & Samuels, 1995; Warren, 1983, among many others). Here we highlight another striking, rarely discussed feature of this distribution: a peak in positive buoyancy flux in the low-latitude Indo-Pacific. This peak is also linked to continental geometry: the equatorial Indo-Pacific (Figure 1c) accounts for the majority of the low-latitude ocean surface area and incurs the majority of surface heat and freshwater fluxes, at these latitudes (consistent with observations, e.g., Grist & Josey, 2003; Large & Yeager, 2009; see supporting information S1).

Crucially, to remain in steady state, the model's interior dynamics must transport buoyancy between remote regions of buoyancy gain and loss. Here we exploit this thermodynamic burden on the system to reassess how the model's Indo-Pacific participates in its GOC. To do so, we derive a theoretical, thermodynamically based *Buoyancy Transport* framework, which uses the global surface buoyancy flux distribution as boundary conditions on the interior GOC state, in section 2. We then apply our framework to unravel global overturning pathways in CESM 1.0 in section 3 and discuss the implications of our model analysis for the real ocean system in section 4.

2. The Buoyancy Transport Framework

We first develop the concept of *buoyancy transport* by extending the methodology behind the heat or salinity functions, which trace oceanic heat and freshwater transports (e.g., Ferrari & Ferreira, 2011; Greatbatch & Zhai, 2007; Zika et al., 2012). We instead apply these methods to buoyancy—the deviation in a water parcel's gravitational acceleration away from it environment depending on temperature, salinity, and pressure. Unlike heat or freshwater fluxes individually, the buoyancy flux field is coupled to the configuration of the residual overturning circulation itself—the circulation along and across density classes (Döös & Webb, 1994; Marshall & Radko, 2003). To demonstrate this coupling most clearly, we make several simplifications. First, we define buoyancy as the departure in a parcel's potential density, ρ, from a global reference density, ρ_0: $b = -\frac{g}{\rho_0}(\rho - \rho_0)$, as referenced to 2000 db pressure and where g is gravity; densities will be expressed as density anomaly $\sigma = \rho - 1000$. We choose this definition despite compelling arguments for defining b with respect to neutral surfaces (e.g., Groeskamp et al., 2017); doing so would be more physically precise but nonconservative (McDougall et al., 2014). Second, we ignore geothermal heating, nonlinearities in the equation of state (EOS), and assume a steady state. These simplifications are made in order to expose novel relationships in the system that emerge when treating buoyancy as a globally conserved tracer. We interpret model behavior from this perspective and leave an analysis of higher-order processes for subsequent work.

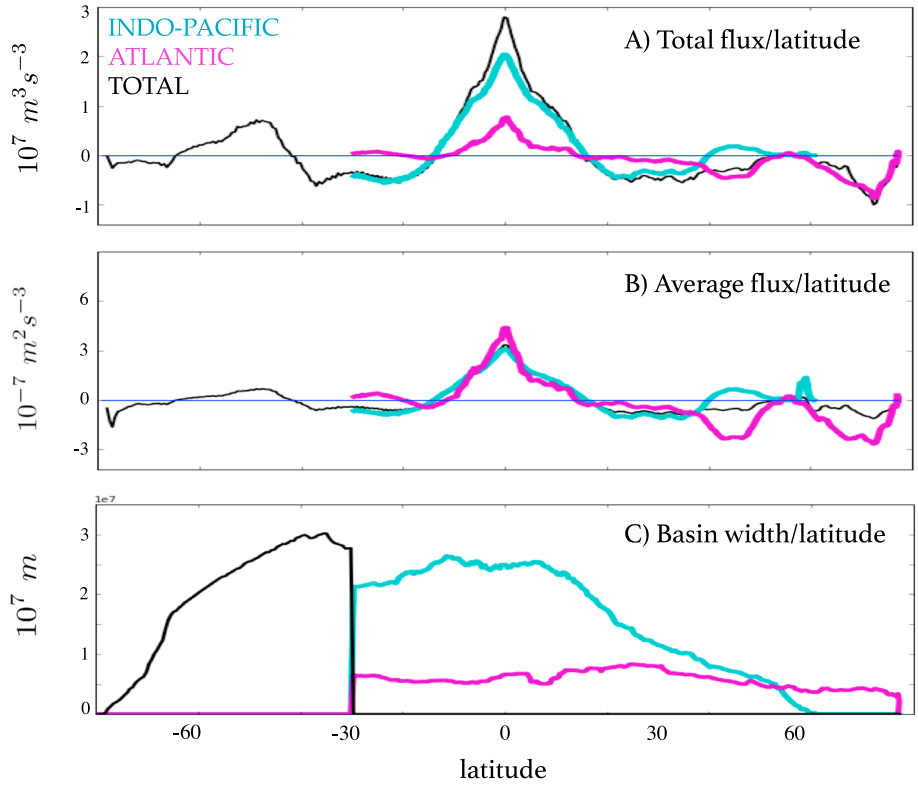

Figure 1. (a) The meridional distribution of the zonally integrated surface buoyancy flux (m^3/s^3) from a preindustrial control simulation in CESM 1.0, representing the global ocean (black), Atlantic Basin (magenta), and the Indo-Pacific Basins (ceylon). The integrated buoyancy flux varies based on both meridional distributions of the zonal-mean buoyancy flux (m^3/s^2) and the total basin width (m) as shown in panels (b) and (c), respectively.

First, consider the volume, $V(\sigma, y)$, composed of all waters denser than σ, between latitude y and the northernmost point in the domain, y_N, and between the eastern and western boundaries of the domain, X_E and X_W,

$$V(\sigma, y) \equiv \int_{-H}^{0}\int_{y}^{y_n}\int_{X_E}^{X_W} \mathcal{H}(\sigma^*(\boldsymbol{x}) - \sigma)\mathrm{d}x\mathrm{d}y\mathrm{d}z. \tag{1}$$

$V(\sigma, y)$ is bounded in the interior by the isopycnal surface S_σ, defined by the depth of σ at each point between latitude y and the location where σ intersects the surface. Here H is the depth of the ocean bottom, $\sigma^*(\boldsymbol{x})$ is the density evaluated at position $\boldsymbol{x}$, and $\mathcal{H}$ is the Heaviside function, where $\mathcal{H}(n) = 1$ for $n \geq 0$ and $\mathcal{H}(n) = 0$ for $n < 0$. Within a closed basin, that is, X_E and X_W coincident with continental boundaries or spanning the circumference of the Earth, $\frac{\mathrm{d}V}{\mathrm{d}t}$ depends only on the meridional transport of waters denser than σ and the convergence of diabatic buoyancy flux, into V, as

$$\frac{\mathrm{d}V}{\mathrm{d}t} = \Psi(y, \sigma) - \frac{\partial}{\partial\sigma}\int_V \mathcal{D}\mathrm{d}V. \tag{2}$$

Term $\Psi(y, \sigma) \equiv -\int_{-H}^{0}\int_{X_E}^{X_W} v(\boldsymbol{x})\mathcal{H}(\sigma'(\boldsymbol{x}) - \sigma)\mathrm{d}x\mathrm{d}z$ quantifies the meridional transport of waters denser than σ, called the isopycnal or residual circulation, where $v(\boldsymbol{x})$ is the local velocity. Term $\mathcal{D} \equiv \frac{D\sigma}{Dt} = -\frac{\rho_0}{g}\nabla\cdot\lambda$ is irreversible density tendency driven by a convergence of diabatic buoyancy flux, λ, with contributions from surface forcing, λ_{surf}, and interior mixing λ_{mix}. Equation (2) quantifies a balance between adiabatic and diabatic volume transport, or *water mass transformation* (Walin, 1982), which is used widely (e.g., Marsh et al., 2000; Nurser et al., 1999; Speer & Tziperman, 1992, among many others) and schematically depicted in Figure S1a. Further, evaluating equation (2) for volume of the global ocean, one discriminates a (residually) adiabatic component of the GOC (e.g., Han et al., 2013; Radko & Kamenkovich, 2011), while the latitudinal divergence of equation (2) parallels equation 3 in Ferrari and Ferreira (2011) and follows from Nurser and Lee (2004).

In this study, we instead explore how this balance relates to buoyancy transport. We consider a steady state and integrate equation (2) with respect to σ, so it simplifies to $\frac{g}{\rho_0}\int_{\sigma'>\sigma}\Psi d\sigma' = -\int_V \nabla\cdot\lambda \mathrm{d}V$. Given our assumptions, diabatic fluxes act only across the volume's interior isopycnal surface and its surface outcrop north of y; further, while S_σ will take on a complex shape, λ_{mix} is always perpendicular to S_σ, so equation (2) becomes

$$\underbrace{\frac{g}{\rho_0}\int_{\sigma'>\sigma}\Psi(\sigma',y)d\sigma'}_{1} = \underbrace{-\int_y^{y_N}\int_{x_E}^{x_W}\lambda_{\mathrm{surf}}\mathcal{H}(\sigma_{\mathrm{surf}}-\sigma)\mathrm{d}x\mathrm{d}y - \int_{S_\sigma}\lambda_{\mathrm{mix}}(\boldsymbol{x})\mathrm{d}S_\sigma}_{2}, \tag{3}$$

where $\sigma_{\mathrm{surf}}(x,y)$ is the sea surface density. Here we have invoked the divergence theorem, $\int_V \nabla\cdot\lambda \mathrm{d}V = \int_S \lambda\cdot\hat{n}\mathrm{d}S$, and S is the bounding surface of $V(\sigma,y)$. Equation (3) exhibits the balance of processes required to avoid a buoyancy tendency within V: the total diabatic buoyancy flux into V (term 2) must be balanced by an adiabatic, advective buoyancy transport (term 1), schematically depicted in Figure S1b. In other words, the residual circulation, Ψ itself, must transport buoyancy. Physically, the flow of relatively light water in one direction must be balanced by the flow of denser water in the opposite direction to conserve volume in a stratified ocean. Together, these opposing flows transport a perturbation in buoyancy along isopycnals and therefore cannot persist without sources and sinks of buoyancy. We introduce a Buoyancy Transport Function, $B(\sigma,y)$ to quantify the total interior buoyancy Ψ transports across y and below a given σ:

$$B(\sigma,y) \equiv \frac{g}{\rho_0}\int_{\sigma'>\sigma}\Psi(\sigma',y)\mathrm{d}\sigma'. \tag{4}$$

Function B is analogous to a broad family of transport functions used to study heat, salinity, and chemical transport (e.g., Iudicone et al., 2011; Ferrari & Ferreira, 2011; Greatbatch & Zhai, 2007; Lund et al., 2011; Zika et al., 2012) except here its streamlines map the interior pathways that buoyancy perturbations take between surface sources and sinks. For this reason, through B we can constrain the structure of the residual circulation itself from the surface buoyancy flux field. We define $\hat{B}(y)$ as the total northward buoyancy transport across latitude y within a closed basin or for the global ocean, which can be calculated independently given either knowledge of the surface buoyancy flux distribution ($\hat{B}_{\mathrm{surf.}}$), or knowledge of the interior circulation and stratification structure ($\hat{B}_{\mathrm{int.}}$),

$$\hat{B}(y) \equiv \underbrace{\frac{g}{\rho_0}\int_{\sigma'>\sigma_{\mathrm{min}}(y)}\Psi(\sigma',y)\mathrm{d}\sigma'}_{\hat{B}_{\mathrm{int.}}} = \underbrace{-\int_y^{y_N}\int_{x_E}^{x_W}\lambda_{\mathrm{surf}}\mathrm{d}x\mathrm{d}y}_{\hat{B}_{\mathrm{surf.}}}, \tag{5}$$

following from equation (3), and where $\sigma_{\mathrm{min}}(y)$ is the minimum density at y. Equation (5) reveals that the *total residual circulation*—integrated across all density classes at a given latitude—must be structured to balance all diabatic surface forcing within the basin to the north, a balance depicted in Figure S1c. Note that the equivalence of $\hat{B}_{\mathrm{int.}}$ and $\hat{B}_{\mathrm{surf.}}$ requires a linear EOS, and will not be perfect in the real ocean or in complex climate models. However, equation (5) elucidates why the GOC depends on surface forcing in each basin: its integral structure provides the oceanic mechanism of redistributing imbalances in surface buoyancy forcing between them.

We adopt this perspective to examine how interior ocean behavior relates to the surface buoyancy flux distribution (Figure 1) in the fully coupled global climate model CESM 1.0, specifically in the final 30 years of the 1,300-year preindustrial (1850s) control run discussed in depth by Gent et al. (2011) and Danabasoglu et al. (2012). The model has 60 vertical layers of varying thicknesses and an average 1° horizontal grid spacing. The effects of transient ocean eddies are parameterized through a spatially varying Gent McWilliams coefficient (e.g., Gent & Danabasoglu, 2011), and this velocity component is included in results below.

3. Application to a Global Climate Model

3.1. Global-Scale Constraints on Ocean Overturning

We begin by evaluating if the model's surface buoyancy flux distribution meaningfully constrains its underlying circulation by comparing $\hat{B}_{\mathrm{surf.}}$ to $\hat{B}_{\mathrm{int.}}$ (equation (5)) in Figure 2. As expected, the surface buoyancy budget does not entirely close, and surface and interior calculations are not perfectly equivalent—we have neglected time-dependent terms and nonlinearities in the EOS. However, their magnitude and large-scale characteristics are encouragingly similar, particularly at low latitudes. In other words, in steady state, the integral

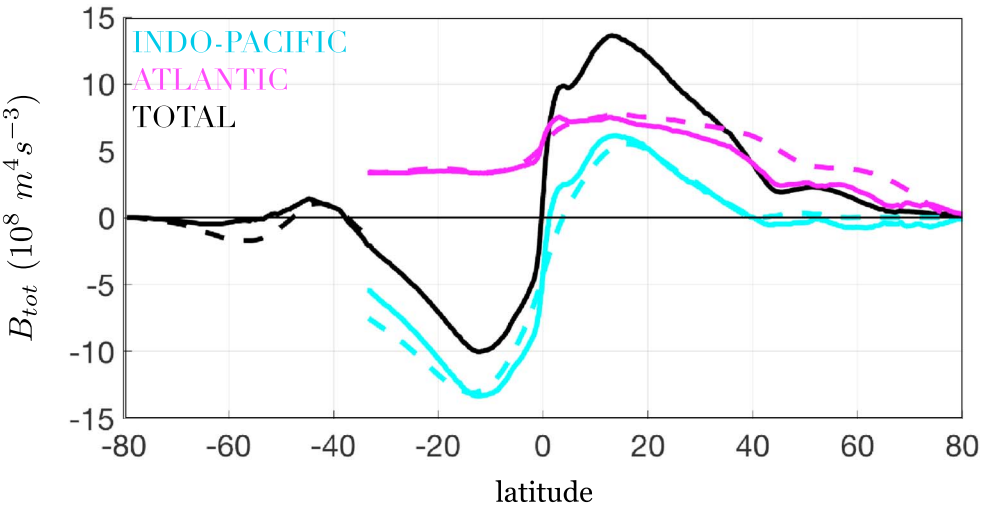

Figure 2. Comparison between $\hat{B}_{\text{int.}}$ (solid lines) and $\hat{B}_{\text{surf.}}$ (dashed lines) [equation (5)] for the global ocean (black), the Atlantic Basin (magenta), and the Indo-Pacific Basins (ceylon).

configuration of Ψ can be constrained from the global surface flux distribution, given no information about interior dynamics. In the Atlantic, meager low-latitude surface buoyancy gains and excessive high-latitude losses require that the basin-scale "total" residual circulation convey buoyancy northward across 30°S (i.e., $\hat{B}_{\text{surf.}}(-30) \approx 3.7 \times 10^8$ m^4/s^3 in the Atlantic) and across all latitudes toward the high-latitude ocean surface. In contrast, in the Indo-Pacific, the total residual circulation must export excess buoyancy out of the low latitudes, poleward into both the Northern and Southern Hemispheres. Despite local redistribution, however, the total surface buoyancy flux integrated over the entire Indo-Pacific basin remains significantly positive; this basin-scale buoyancy surplus must be exported southward across 30°S (i.e., $\hat{B}_{\text{surf.}}(-30) \approx -7.5 \times 10^8$ m^4/s^3 in the Indo-Pacific). Finally, in the Southern Ocean the partial cancelation of regional positive and negative buoyancy fluxes implies that the total residual circulation at 30°S is relatively small, in the circumpolar integral (here $\hat{B}_{\text{surf.}}(-30) \approx 2.3 \times 10^8$ m^4/s^3). However, in the Southern Ocean, Ψ must depart significantly from its zonal mean in order to the satisfy thermodynamic requirements of the basins to its north. Specifically, to facilitate buoyancy transport between the Atlantic and Indo-Pacific Oceans, as well as from each basin to distinct regions of the Southern Ocean surface, there must be a zonal component of the residual circulation, Ψ, south of 30°S. While we can infer fundamental zonal structure in the Southern Ocean from thermodynamics alone, our finding is corroborated by observations of water mass properties, most recently Talley (2013), and by dynamical arguments (Cessi & Jones, 2017; Ferrari et al., 2017; Thompson et al., 2016).

3.2. Interior Implications of Surface Constraints

To understand how the model's overturning circulation accommodates surface buoyancy flux constraints (Figure 2), we first examine the model's overturning streamfunction Ψ in Figure 3. Two vigorous subtropical circulations dominate the globally integrated circulation of low density waters ($\sigma_2 < 35.4$ in Figure 3a). Denser waters ($\sigma_2 > 35.4$) appear to circulate meridionally in two counterrotating cells—often termed the *Upper* and *Lower Cell*. However, this zonally summed structure hides highly distinct and interwoven basin-scale circulations, complexity anticipated from previous work (Broecker, 1991; Gordon, 1986; Lumpkin & Speer, 2007; Schmitz, 1996; Talley, 2013) and inferred here from thermodynamic arguments. While buoyancy constraints require a zonal residual circulation in the Southern Ocean, as noted above, deciphering this structure is beyond the scope of this study. Instead, we focus on the northern basins, particularly because these basins are subject to significant and opposing residuals in basin-scale surface buoyancy flux.

The Atlantic circulation (Figure 3b) is dominated by a strong clockwise cell, associated with the formation of NADW and its export into the Southern Ocean, a structure often termed the Atlantic meridional overturning circulation. A weak secondary circulation involving the inflow, transformation, and outflow of Southern Ocean-sourced Antarctic bottom waters occurs across $\sigma_2 > 37.25$.

The Indo-Pacific circulation differs greatly from the Atlantic (Figure 3c). The circulation and transformation of both dense bottom waters ($\sigma_2 > 37.25$) and light thermocline waters ($\sigma_2 < 35.4$) is strongest within

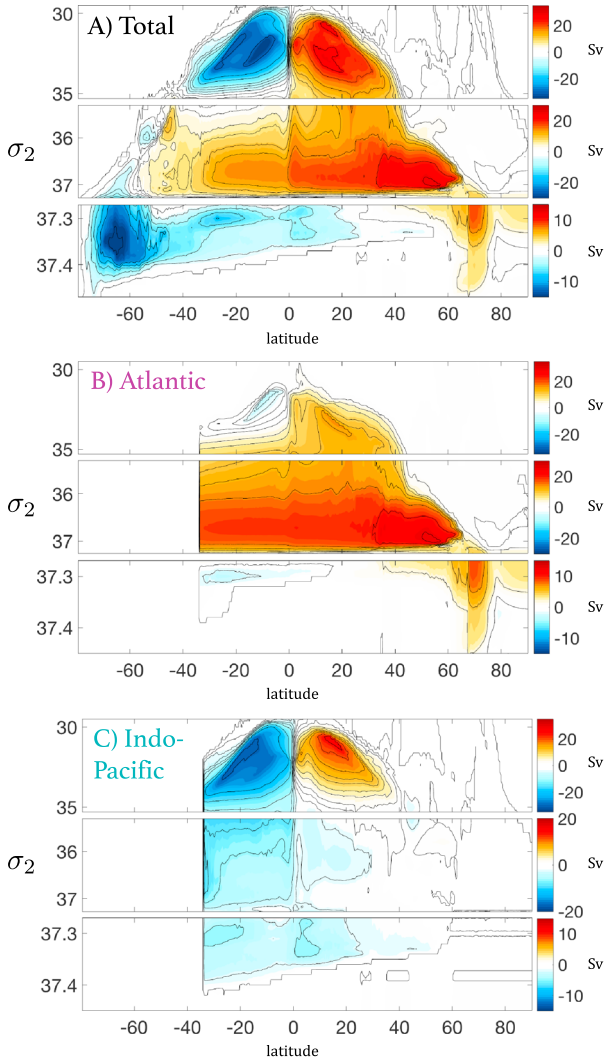

Figure 3. Isopycnal (*residual*) overturning circulation, Ψ (Sv), summed (a) globally; (b) across the Atlantic, and (c) Indo-Pacific. The spacing of σ_2 varies to resolve details in surface, intermediate, and abyssal circulations.

these basins. Notably, a third circulation emerges between the abyssal and near-surface circulation branches, strongest within the Southern Hemisphere and spanning deep water classes ($35.4 < \sigma_2 < 37.25$), in other words, depicting substantial inflow of water masses at equivalent densities to those flowing out of the Atlantic. Comparing Ψ across 30°S between basins reveals that ≈45% of NADW (defined from circulation features here as $37.2 \leq \sigma_2 \leq 36.5$) flows from the Atlantic into the Indo-Pacific without any residual transformation in the Southern Ocean. Instead, inflowing NADW-like waters are destroyed through mixing with thermocline waters and equatorial upwelling in the Indo-Pacific. These processes are manifested as uninterrupted streamlines of Ψ, curving across deep water classes up into the surface gyres near the equator in Figure 3c. This deep circulation is consistent with a zonally summed projection of the interbasin *warm route* or conveyor belt, argued for by Gordon (1986) and Broecker (1987). We henceforth refer to it as the *interbasin* circulation, meant in a thermodynamic sense, though its zonal details are beyond our scope. Bear in mind, the canonical observationally based circulation inversion of Lumpkin and Speer (2007) shows little direct interbasin transport. Instead, they find that waters flowing into the deep and abyssal Indo-Pacific are denser than those flowing out of the Atlantic, and therefore, they infer a significantly stronger global abyssal overturning branch than shown here, at 20.9 ± 4.9 Sv. However, recent dynamical arguments propose interbasin flows may be greater than often assumed (Cessi & Jones, 2017; Ferrari et al., 2017). We discuss how these model biases impact our conclusions in Section 4.

Here, however, our goal is not to evaluate model fidelity but to demonstrate how its simulated surface buoyancy flux distribution relates to its circulation through the lens of buoyancy transport. As described in section 2, $B(\sigma, y)$ quantifies the cumulative buoyancy transport sustained by the circulation of all waters denser than water mass σ. To illustrate the spatial configuration of B in relation to Ψ, we project both fields onto time- and zonal-mean isopycnal depths in each basin (Figure 4). Streamlines of B represent the total meridional buoyancy transport between the sea floor and a particular depth at each latitude and should be interpreted as the average interior buoyancy transport pathways supported by Ψ. Again, we focus our analysis on distinctions between the Atlantic and Indo-Pacific, given their opposing basin-scale residuals in surface buoyancy flux. In the Atlantic, the coupled structures of Ψ and B reveal that the dominant clockwise *Atlantic meridional overturning circulation* transports buoyancy into the basin, and across all latitudes, to be lost from the high-latitude surface. Physically, this transport is supported by the northward (southward) flow of lighter (denser) water masses across all latitudes, in turn supported by local surface buoyancy loss and compensating remote surface buoyancy gain.

The structure of B in the Indo-Pacific sheds light on how its basin-scale surplus in positive surface buoyancy flux is transported from the basin. Near the surface, vigorous subtropical gyre circulations acting across highly stratified waters, efficiently redistribute buoyancy from low latitude to midlatitude, as anticipated from previous analyses of oceanic heat transport (e.g., Ferrari & Ferreira, 2011). Thermocline transport (above ~400 m on average) accounts for the meridionally symmetric component of $\hat{B}$, and additionally, half of the total buoyancy transport southward from the Indo-Pacific at 30°, as warm surface waters leak from the basin to be modified in the Atlantic and Southern Oceans.

Nonetheless, approximately half of the basin-scale surplus, $\hat{B}_{|30S}$, remains to be transported from the basin by the circulation below. In this model, this transport is predominately sustained by the interbasin circulation between 400- and 3,500-m depth and associated with densities of $35.4 < \sigma_2 < 37.25$. Streamlines of B clarify how this process relates to surface forcing: a positive surface buoyancy flux, predominately at low latitudes in the Southern Hemisphere of the Indo-Pacific, lightens upwelling near-surface waters. This

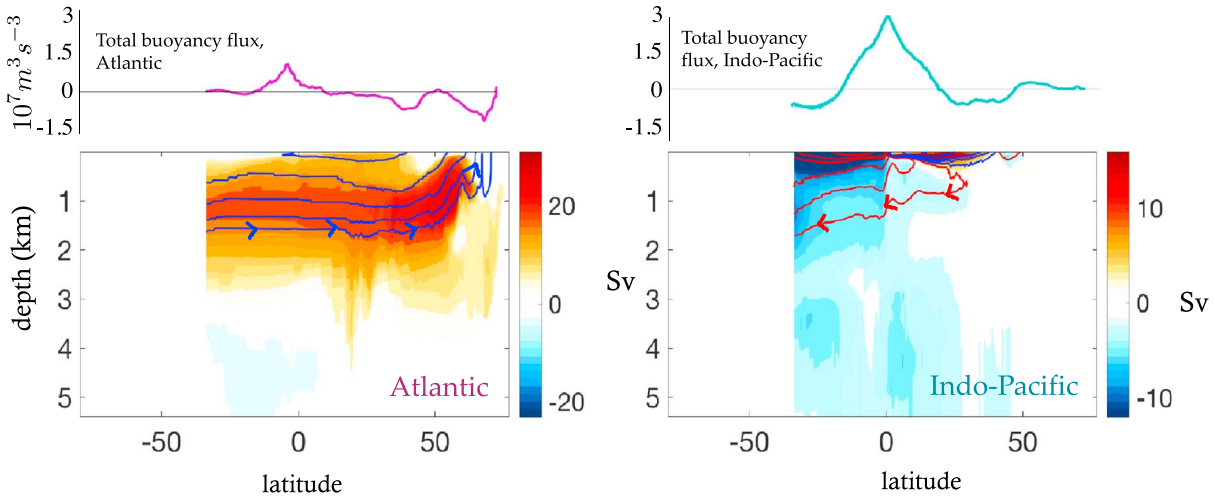

Figure 4. (bottom panels) The $\Psi(\sigma, y)$ (shaded color contours) and $B(\sigma, y)$ (overlaid red and blue contours) in the Atlantic (left) and Indo-Pacific basins (right) and projected onto mean isopycnal depths. Note, contours of B are colored and annotated with arrows to denote the direction of buoyancy transport (red = clockwise, blue = counterclockwise); streamlines of B start from (terminate at) surface regions of net positive (negative) buoyancy flux, illustrated in the top panels and equivalent to Figure 1a. Contours separate intervals of 20% $\hat{B}$ in the Atlantic and of ≈17% $\hat{B}$ in the Indo-Pacific.

perturbation is effectively *transported* into the interior through mixing between subtropical thermocline waters and intermediate waters below and the adiabatic sliding of water masses along tilted isopycnals. This positive buoyancy perturbation is then conveyed southward across 30°S, supported by the inflow of denser NADW classes and outflow of lighter intermediate waters. In this model, meridional buoyancy transport in the abyssal ocean is negligible since the abyssal circulation is relatively weak and acts across minimal stratification: only 1% of $\hat{B}_{|30S}$ occurs below 3,500 m (associated with $\sigma_2 > 37.25$), though it is probable that this model underestimates abyssal buoyancy transport given the biases in its abyssal circulation. In a case more consistent with Lumpkin and Speer (2007), for instance, a stronger (weaker) abyssal (interbasin) circulation in the Indo-Pacific would require greater abyssal (reduced deep) water mass transformation north of 30°S within the basin, and stronger abyssal (weaker deep) southward buoyancy transport across 30°S. In this case, streamlines in B would stretch further into the abyss before curving out of the basin than those represented in Figure 4 and would likely involve convoluted zonal pathways between basins in the Southern Ocean (e.g., Talley, 2013). Critically, however, our primary point remains the same: this scenario equivalently requires coupling in the Indo-Pacific between thermocline, deep, and abyssal dynamics to sustain buoyancy transport into its abyss and out of its southern boundary. In other words, streamlines in B must ultimately begin and end at the surface.

4. Discussion and Conclusions

In this study, we demonstrate that the GOC is itself the oceanic mechanism to redistribute imbalances in surface buoyancy flux between ocean basins; it is therefore inextricably coupled to, and quantifiably constrained by, the global surface buoyancy flux distribution. Despite historic emphasis on the importance of surface forcing in the Southern and North Atlantic Oceans (Bell, 2015; Gnanadesikan, 1999; Jansen & Nadeau, 2016; Klinger & Marotzke, 1999; Marotzke & Klinger, 2000; Marshall & Speer, 2012; Nikurashin & Vallis, 2011, 2012; Radko & Kamenkovich, 2011; Samelson, 2009; Wolfe & Cessi, 2011), the steady state GOC must be equally constrained by surface buoyancy fluxes everywhere. Ultimately, ocean overturning must export and destroy the global dense waters formed in excess in the high latitudes of the Atlantic and Southern Oceans; however, it must simultaneously export and destroy the global *light waters* formed in excess in the expansive low-latitude Indo-Pacific.So long as the Indo-Pacific gains more buoyancy than it looses, the GOC cannot conceptualized as a *deep* system, decoupled from shallower ocean dynamics; instead, this circulation involves the entire global ocean.

We present a thermodynamically based perspective on the GOC that highlights potential limitations in many conceptual or idealized ocean models, particularly in their treatment of Indo-Pacific processes. For instance, abyssal Indo-Pacific mixing bears a widely appreciated, comprehensively explored influence on overturning

dynamics (e.g., De Lavergne et al., 2017; Ferrari et al., 2016; Mashayek et al., 2015). However, abyssal mixing is considered the singular influential Indo-Pacific process in many idealized ocean models, while Indo-Pacific surface fluxes and shallow ocean dynamics are expected to adjust passively to the requirements of abyssal dynamics (e.g., Ferrari et al., 2014; Nikurashin & Vallis, 2011, 2012; Radko & Kamenkovich, 2011; Thompson et al., 2016). As a consequence, significant emphasis has been placed on the role of Southern Ocean surface forcing in mediating the overturning circulation to its north (e.g., Ferrari et al., 2014; Sun et al., 2018; Thompson et al., 2016), particularly so in frameworks that consider the Southern Ocean and global circulation to be zonally symmetric (Bell, 2015; Gnanadesikan, 1999; Jansen, 2017; Jansen & Nadeau, 2016; Klinger & Marotzke, 1999; Marotzke & Klinger, 2000; Nikurashin & Vallis, 2011, 2012; Radko & Kamenkovich, 2011; Samelson, 2009; Shakespeare & Hogg, 2012; Wolfe & Cessi, 2011).

However, our analysis of buoyancy transport in the fully coupled climate model CESM 1.0 supports a more nuanced view. In this model, the Indo-Pacific basin receives a significant surplus in positive surface buoyancy flux. This basin-scale surface forcing pattern requires that Indo-Pacific thermocline processes be coupled to processes in the Atlantic and Southern Oceans, since this surplus in buoyancy must be lost remotely in a steady state. blackFurther, the global buoyancy flux distribution requires key zonal asymmetry in the circulation south of 30°S, without which buoyancy transport between the basins to its north cannot occur. Our thermodynamic arguments align with previous work emphasizing the dynamical importance of a *warm route* between Indo-Pacific and Atlantic Oceans (e.g., Beal et al., 2011; Broecker, 1991; Cessi & Jones, 2017; Donners & Drijfhout, 2004; Gordon, 1986) and of zonal asymmetries in the Southern Ocean residual circulation (e.g.,Ferrari et al., 2014, 2017; Talley, 2013; Thompson et al., 2016).

Of course, the surface buoyancy flux distribution analyzed here is highly influenced by oceanic and atmospheric dynamics; inevitably, its details diverge from the real ocean. However, our primary conclusions follow from basin-scale differences in surface fluxes and buoyancy transports, differences that are qualitatively corroborated by observations (e.g., Ganachaud & Wunsch, 2003; Grist & Josey, 2003; Trenberth & Caron, 2001), as discussed further in the supporting information S1. The specific model dynamics that support interior buoyancy transport, however, are subject to important caveats, particularly in the deep Indo-Pacific. As discussed in section 3, the abyssal circulation is much weaker than observational estimates, while the direct *interbasin* circulation is too strong. Significant biases in abyssal properties are common in standard resolution climate models: key bottom water formation processes are not resolved (Heuzé et al., 2013; Newsom et al., 2016), and dense waters are often destroyed too quickly as a result of spurious explicit and numerical diffusion (Farneti et al., 2015; Griffies et al., 2000; Newsom et al., 2016). Conceivably, the dominance of the interbasin circulation described here results from abyssal biases or from similar biases in unphysical upper ocean mixing. However, direct evaluation of the full-depth Indo-Pacific streamfunction against Lumpkin and Speer (2007) warrants care: the authors note that their methods do not faithfully resolve upper ocean dynamics. Further, Donners and Drijfhout (2004) argue that common inversion techniques, including those used by Lumpkin and Speer (2007), drastically underestimate the volume of warm Indo-Pacific-surface waters that flow into the Atlantic. Most importantly, despite the model's inherent limitations, it exemplifies that a residual overturning circulation must transport buoyancy around the global ocean to balance a heterogeneous surface buoyancy forcing. This means that any exterior constraints on the surface buoyancy flux distribution must constrain the GOC, notable, given that the Indo-Pacific accounts for the majority of the global ocean's low-latitude surface area (Figure 1c). Arguably, its distinct geometry may predispose the Indo-Pacific to serve as a buoyancy source to the global ocean, reinforcing zonal asymmetry in surface buoyancy forcing between basins, across a range of climate states. While similar exterior Atlantic and Southern Ocean constraints have been argued for extensively (e.g., Czaja, 2009; De Boer et al., 2008; Ferreira et al., 2010, 2018; Jones et al., 2017; Marshall & Radko, 2003; Nilsson et al., 2013; Toggweiler & Samuels, 1995; Warren, 1983; Weaver et al., 1999), here we emphasize that any potential geometrical constraints or any influence of processes outside of the ocean, upon Indo-Pacific surface forcing, must equally be accommodated by the organization of the GOC.

By construction, our arguments apply to a steady state system. However, they raise important questions about low-latitude controls on GOC dynamics. The low-latitude Indo-Pacific is the most variable region of the ocean's surface over interannual time scales (e.g., Philander, 1983). However, the possibility that associated variations in buoyancy forcing and/or mixing across the thermocline directly modulate global overturning through interior oceanic pathways (without invoking atmospheric teleconnections) is critically underexplored. Note, these regional variations could manifest in GOC variability at time scales longer than their interannual origin and shorter than the Pacific's characteristic diffusive time scale. Instead, they could be *reddened* by the

advective-diffusive dynamics of interbasin flows (e.g., Roe, 2009), possibly giving rise to global variability over decadal or centennial time scales. Finally, our results are relevant to the ocean's evolution between distinct climate states (e.g., Ferrari et al., 2014). Specifically, we emphasize that regardless of extreme shifts in high-latitude processes during transient climate evolution, any equilibrated ocean state is ultimately constrained by low-latitude processes—changes in high-latitude buoyancy loss must be accommodated by low-latitude buoyancy gains. Considerations of low-latitude glacial-interglacial dynamics could add nuance to our understanding of climate shifts, and possible oceanic states, in the past and future.

Acknowledgments
We thank Igor Kamenkovich, an anonymous reviewer, and the Editor for constructive suggestions, and Cecilia Bitz, Jess Adkins, Frank Bryan, and Lynne Talley for helpful discussions. This work was funded by the National Oceanic and Atmospheric Administration (NOAA) CGC Fellowship (E. R. N.) and by the National Science Foundation (NSF) grant OCE-1235488 (A. F. T.). Output from the simulation used is available for download at http://www.cesm.ucar.edu/experiments/cesm1.0/.

References

Beal, L. M., Ruijter, W. P. M. D., Biastoch, A., Zahn, R., Wcrp, S., & Working, I. (2011). On the role of the Agulhas system in ocean circulation and climate. *Nature*, *472*(7344), 429–436. https://doi.org/10.1038/nature09983

Bell, M. J. (2015). Meridional overturning circulations driven by surface wind and buoyancy forcing. *Journal of Physical Oceanography*, *45*(11), 2701–2714. https://doi.org/10.1175/JPO-D-14-0255.1

Broecker, W. (1987). The biggest chill. *Natural History*, *56*, 74–82.

Broecker, W. (1991). The great ocean conveyor. *Oceanography*, *4*(2), 79–89. https://doi.org/10.5670/oceanog.1991.07

Cessi, P., & Jones, C. S. (2017). Warm-route versus cold-route interbasin exchange in the meridional overturning circulation. *Journal of Physical Oceanography*, *47*(8), 1981–1997. https://doi.org/10.1175/JPO-D-16-0249.1

Czaja, A. (2009). Atmospheric control on the thermohaline circulation. *Journal of Physical Oceanography*, *39*(1), 234–247. https://doi.org/10.1175/2008JPO3897.1

Danabasoglu, G., Bates, S. C., Briegleb, B. P., Jayne, S. R., Jochum, M., Large, W. G., et al. (2012). The CCSM4 ocean component. *Journal of Climate*, *25*, 1361–1389. https://doi.org/10.1175/JCLI-D-11-00091.1

De Boer, A. M., Toggweiler, J. R., & Sigman, D. M. (2008). Atlantic dominance of the meridional overturning circulation. *Journal of Physical Oceanography*, *38*(2), 435–450. https://doi.org/10.1175/2007JPO3731.1

De Lavergne, C., Madec, G., Roquet, F., Holmes, R. M., & McDougall, T. J. (2017). Abyssal ocean overturning shaped by seafloor distribution. *Nature*, *551*(7679), 181–186. https://doi.org/10.1038/nature24472

Donners, J., & Drijfhout, S. S. (2004). The Lagrangian view of South Atlantic interocean exchange in a global ocean model compared with inverse model results. *Journal of Physical Oceanography*, *34*(5), 1019–1035. https://doi.org/10.1175/1520-0485(2004)034<1019:TLVOSA>2.0.CO;2

Döös, K., & Webb, D. J. (1994). The Deacon Cell and other meridional cells of the Southern Ocean. *Journal of Physical Oceanography*, *24*, 429–442. https://doi.org/10.1175/1520-0485(1994)024<0429:TDCATO>2.0.CO;2

Farneti, R., Downes, S. M., Griffies, S. M., Marsland, S. J., Behrens, E., Bentsen, M., et al. (2015). An assessment of Antarctic Circumpolar Current and Southern Ocean meridional overturning circulation during 1958–2007 in a suite of interannual CORE-II simulations. *Ocean Modelling*, *93*, 84–120. https://doi.org/10.1016/j.ocemod.2015.07.009

Ferrari, R., & Ferreira, D. (2011). What processes drive the ocean heat transport? *Ocean Modelling*, *38*(3-4), 171–186. https://doi.org/10.1016/j.ocemod.2011.02.013

Ferrari, R., Jansen, M. F., Adkins, J. F., Burke, A., Stewart, A. L., & Thompson, A. F. (2014). Antarctic sea ice control on ocean circulation in present and glacial climates. *Proceedings of the National Academy of Sciences of the United States of America*, *111*(24), 8753–8758. https://doi.org/10.1073/pnas.1323922111

Ferrari, R., Mashayek, A., McDougall, T. J., Nikurashin, M., & Campin, J.-M. (2016). Turning ocean mixing upside down. *Journal of Physical Oceanography*, *46*(7), 2239–2261. https://doi.org/10.1175/JPO-D-15-0244.1

Ferrari, R., Nadeau, L.-P., Marshall, D. P., Allison, L. C., & Johnson, H. L. (2017). A model of the ocean overturning circulation with two closed basins and a reentrant channel. *Journal of Physical Oceanography*, *47*(12), 2887–2906. https://doi.org/10.1175/JPO-D-16-0223.1

Ferreira, D., Cessi, P., Coxall, H. K., De Boer, A., Dijkstra, H. A., Drijfhout, S. S., et al. (2018). Atlantic-Pacific asymmetry in deep water formation. *Annual Review of Earth and Planetary Sciences*, *46*, 327–52. https://doi.org/10.1146/annurev-earth-082517

Ferreira, D., Marshall, J., & Campin, J.-M. (2010). Localization of deep water formation: Role of atmospheric moisture transport and geometrical constraints on ocean circulation. *Journal of Climate*, *23*(6), 1456–1476. https://doi.org/10.1175/2009JCLI3197.1

Ganachaud, A., & Wunsch, C. (2003). Large-scale ocean heat and freshwater transports during the world ocean circulation experiment. *Journal of Climate*, *16*(4), 696–705. https://doi.org/10.1175/1520-0442(2003)016<0696:LSOHAF>2.0.CO;2

Gent, P. R., & Danabasoglu, G. (2011). Response to increasing Southern Hemisphere winds in CCSM4. *Journal of Climate*, *24*(19), 4992–4998. https://doi.org/10.1175/JCLI-D-10-05011.1

Gent, P. R., Danabasoglu, G., Donner, L. J., Holland, M. M., Hunke, E. C., Jayne, S. R., et al. (2011). The Community Climate System model version 4. *Journal of Climate*, *24*(19), 4973–4991. https://doi.org/10.1175/2011JCLI4083.1

Gnanadesikan, A. (1999). A simple predictive model for the structure of the oceanic pycnocline. *Science*, *283*(5410), 2077–2079. https://doi.org/10.1126/science.283.5410.2077

Gordon, A. L. (1986). Interocean exchange of thermocline water. *Journal of Geophysical Research*, *91*(C4), 5037. https://doi.org/10.1029/JC091iC04p05037

Greatbatch, R. J., & Zhai, X. (2007). The generalized heat function. *Geophysical Research Letters*, *34*, L21601. https://doi.org/10.1029/2007GL031427

Griffies, S. M., Pacanowski, R. C., & Hallberg, R. W. (2000). Spurious diapycnal mixing associated with advection in a z-coordinate ocean model. *Monthly Weather Review*, *128*, 538–564. https://doi.org/10.1175/1520-0493(2000)128<0538:SDMAWA>2.0.CO;2

Grist, J. P., & Josey, S. A. (2003). Inverse analysis adjustment of the SOC air-sea flux climatology using ocean heat transport constraints. *Journal of Climate*, *16*, 3274–3295. https://doi.org/10.1175/1520-0442(2003)016<3274:IAAOTS>2.0.CO;2

Groeskamp, S., Sloyan, B. M., Zika, J. D., & McDougall, T. J. (2017). Mixing inferred from an ocean climatology and surface fluxes. *Journal of Physical Oceanography*, *47*(3), 667–687. https://doi.org/10.1175/JPO-D-16-0125.1

Han, M., Kamenkovich, I., Radko, T., & Johns, W. E. (2013). Relationship between air-sea density flux and isopycnal meridional overturning circulation in a warming climate. *Journal of Climate*, *26*(8), 2683–2699. https://doi.org/10.1175/JCLI-D-11-00682.1

Heuzé, C., Heywood, K. J., Stevens, D. P., & Ridley, J. K. (2013). Southern Ocean bottom water characteristics in CMIP5 models. *Geophysical Research Letters*, *40*, 1409–1414. https://doi.org/10.1002/grl.50287

Iudicone, D., Rodgers, K. B., Stendardo, I., Aumont, O., Madec, G., Bopp, L., et al. (2011). Water masses as a unifying framework for understanding the Southern Ocean carbon cycle. *Biogeosciences*, *8*(5), 1031–1052. https://doi.org/10.5194/bg-8-1031-2011

Jansen, M. F. (2017). Glacial ocean circulation and stratification explained by reduced atmospheric temperature. *Proceedings of the National Academy of Sciences*, *114*(1), 45–50. https://doi.org/10.1073/pnas.1610438113

Jansen, M. F., & Nadeau, L.-P. (2016). The effect of Southern Ocean surface buoyancy loss on the deep-ocean circulation and stratification. *Journal of Physical Oceanography*, *46*(11), 3455–3470. https://doi.org/10.1175/JPO-D-16-0084.1

Jones, C. S., Cessi, P., Jones, C. S., & Cessi, P. (2017). Size matters: Another reason why the Atlantic is saltier than the Pacific. *Journal of Physical Oceanography*, *47*, 17–0075. https://doi.org/10.1175/JPO-D-17-0075.1

Klinger, B. A., & Marotzke, J. (1999). Behavior of double-hemisphere thermohaline flows in a single basin. *Journal of Physical Oceanography*, *29*(3), 382–399. https://doi.org/10.1175/1520-0485(1999)029<0382:BODHTF>2.0.CO;2

Large, W. G., & Yeager, S. G. (2009). The global climatology of an interannually varying air-sea flux data set. *Climate Dynamics*, *33*, 341–364. https://doi.org/10.1007/s00382-008-0441-3

Lumpkin, R., & Speer, K. (2007). Global ocean meridional overturning. *Journal of Physical Oceanography*, *37*(10), 2550–2562. https://doi.org/10.1175/JPO3130.1

Lund, D. C., Adkins, J. F., & Ferrari, R. (2011). Abyssal Atlantic circulation during the Last Glacial Maximum: Constraining the ratio between transport and vertical mixing. *Paleoceanography*, *26*, PA1213. https://doi.org/10.1029/2010PA001938

Marotzke, J., & Klinger, B. A. (2000). The dynamics of equatorially asymmetric thermohaline circulations. *Journal of Physical Oceanography*, *30*(5), 955–970. https://doi.org/10.1175/1520-0485(2000)030<0955:TDOEAT>2.0.CO;2

Marsh, R., Nurser, A., Megann, A., & New, A. (2000). Water mass transformation in the Southern Ocean of a global isopycnal coordinate GCM. *Journal of Physical Oceanography*, *30*(5), 1013–1045. https://doi.org/10.1175/1520-0485(2000)030<1013:WMTITS>2.0.CO;2

Marshall, J., & Radko, T. (2003). Residual-mean solutions for the Antarctic circumpolar current and its associated overturning circulation. *Journal of Physical Oceanography*, *33*(11), 2341–2354. https://doi.org/10.1175/1520-0485(2003)033<2341:RSFTAC>2.0.CO;2

Marshall, J., & Speer, K. (2012). Closure of the meridional overturning circulation through Southern Ocean upwelling. *Nature Geoscience*, *5*(3), 171–180. https://doi.org/10.1038/ngeo1391

Mashayek, A., Ferrari, R., Nikurashin, M., & Peltier, W. R. (2015). Influence of enhanced abyssal diapycnal mixing on stratification and the ocean overturning circulation. *Journal of Physical Oceanography*, *45*(10), 2580–2597. https://doi.org/10.1175/JPO-D-15-0039.1

McDougall, T. J., Groeskamp, S., & Griffies, S. M. (2014). On geometrical aspects of interior ocean mixing. *Journal of Physical Oceanography*, *44*(8), 2164–2175. https://doi.org/10.1175/JPO-D-13-0270.1

Munk, W. H. (1966). Abyssal recipes. *Deep Sea Research and Oceanographic Abstracts*, *13*(4), 707–730. https://doi.org/10.1016/0011-7471(66)90602-4

Newsom, E. R., Bitz, C. M., Bryan, F. O., Abernathey, R., & Gent, P. R. (2016). Southern Ocean deep circulation and heat uptake in a high-resolution climate model. *Journal of Climate*, *29*, 2597–2619. https://doi.org/10.1175/JCLI-D-15-0513.1

Nikurashin, M., & Vallis, G. (2011). A theory of deep stratification and overturning circulation in the ocean. *Journal of Physical Oceanography*, *41*(3), 485–502. https://doi.org/10.1175/2010JPO4529.1

Nikurashin, M., & Vallis, G. (2012). A theory of the interhemispheric meridional overturning circulation and associated stratification. *Journal of Physical Oceanography*, *42*(10), 1652–1667. https://doi.org/10.1175/JPO-D-11-0189.1

Nilsson, J., Langen, P. L., Ferreira, D., & Marshall, J. (2013). Ocean basin geometry and the salinification of the Atlantic Ocean. *Journal of Climate*, *26*(16), 6163–6184. https://doi.org/10.1175/JCLI-D-12-00358.1

Nurser, A., & Lee, M. (2004). Isopycnal averaging at constant height. Part I: The formulation and a case study. *Journal of physical oceanography*, 2721–2739. https://doi.org/10.1175/JPO2650.1

Nurser, A. J. G., Marsh, R., & Williams, R. G. (1999). Diagnosing water mass formation from air-sea fluxes and surface mixing. *Journal of Physical Oceanography*, *29*(7), 1468–1487. https://doi.org/10.1175/1520-0485(1999)029<1468:DWMFFA>2.0.CO;2

Philander, S. (1983). El Niño/Southern Oscillation phenomena. *Nature*, *302*, 295–301. https://doi.org/10.1038/302295a0

Radko, T., & Kamenkovich, I. (2011). Semi-adiabatic model of the deep stratification and meridional overturning. *Journal of Physical Oceanography*, *41*(4), 757–780. https://doi.org/10.1175/2010JPO4538.1

Roe, G. (2009). Feedbacks, timescales, and seeing red. *Annual Review of Earth and Planetary Sciences*, *37*(1), 93–115. https://doi.org/10.1146/annurev.earth.061008.134734

Samelson, R. M. (2009). A simple dynamical model of the warm-water branch of the middepth meridional overturning cell. *Journal of Physical Oceanography*, *39*(5), 1216–1230. https://doi.org/10.1175/2008JPO4081.1

Schmitz, W. J. (1996). On the world ocean circulation: Volume II. Whoi-96-08, II(December), doi:10.1575/1912/356.

Shakespeare, C. J., & Hogg, A. (2012). An analytical model of the response of the meridional overturning circulation to changes in wind and buoyancy forcing. *Journal of Physical Oceanography*, *42*(8), 1270–1287. https://doi.org/10.1175/JPO-D-11-0198.1

Speer, K., & Tziperman, E. (1992). Rates of water mass formation in the North Atlantic Ocean. *Journal of Physical Oceanography*, *22*(1), 93–104. https://doi.org/10.1175/1520-0485(1992)022<0093:ROWMFI>2.0.CO;2

Stommel, H. (1961). Thermohahe convection with two stable regimes of flow. https://doi.org/10.1111/j.2153-3490.1961.tb00079.x

Sun, S., Eisenman, I., & Stewart, A. L. (2018). Does Southern Ocean surface forcing shape the global ocean overturning circulation? *Geophysical Research Letters*, *45*, 2413–2423. https://doi.org/10.1002/2017GL076437

Talley, L. (2013). Closure of the global overturning circulation through the Indian, Pacific, and Southern Oceans: Schematics and transports. *Oceanography*, *26*(1), 80–97. https://doi.org/10.5670/oceanog.2011.65

Thompson, A. F., Stewart, A. L., & Bischoff, T. (2016). A Multibasin residual-mean model for the global overturning circulation. *Journal of Physical Oceanography*, *46*(9), 2583–2604. https://doi.org/10.1175/JPO-D-15-0204.1

Toggweiler, J. R., & Samuels, B. (1995). Effect of drake passage on the global thermohaline circulation. *Deep-Sea Research Part I*, *42*(4), 477–500. https://doi.org/10.1016/0967-0637(95)00012-U

Trenberth, K. E., & Caron, J. M. (2001). Estimates of meridional atmosphere and ocean heat transports. *Journal of Climate*, *14*(16), 3433–3443. https://doi.org/10.1175/1520-0442(2001)014<3433:EOMAAO>2.0.CO;2

Walin, B. G. (1982). On the relation between sea-surface heat flow and thermal circulation in the ocean. *Tellus*, *32*, 187–195.

Warren, B. A. (1983). Why is no deep water formed in the North Pacific? *Journal of Marine Research*, *41*, 327–347.

Weaver, a. J., Bitz, C. M., Fanning, A. F., & Holland, M. M. (1999). Thermohaline circulation: High-latitude phenomena and the difference between the Pacific and Atlantic. *Annual Review of Earth and Planetary Sciences*, *27*(1), 231–285. https://doi.org/10.1146/annurev.earth.27.1.231

Wolfe, C. L., & Cessi, P. (2011). The adiabatic pole-to-pole overturning circulation. *Journal of Physical Oceanography*, *41*(9), 1795–1810. https://doi.org/10.1175/2011JPO4570.1

Zika, J. D., England, M. H., & Sijp, W. P. (2012). The ocean circulation in thermohaline coordinates. *Journal of Physical Oceanography*, *42*(5), 708–724. https://doi.org/10.1175/JPO-D-11-0139.1